

Wear and Impact Behavior of Ductile Cast Iron at different CE and Cast Thickness

A.M. Omran¹, G.T. Abdel-Jaber², and A. A. Gonim²

1. Mining and petroleum Dept., Faculty of Engineering –Qena, AL-AZhar University, Qena, Egypt
 2. Mechanical engineering Dept., Faculty of engineering, South Valley University, Qena, Egypt.
- Corresponding Author : mranasser@hotmail.com

Abstract—Spheroidal Graphite Iron (SGI) has a better mechanical properties, good castability, machinability and thermal resistance. It emerged as replacement to other types of cast iron owing to some specific applications. The present research studies the wear and impact of the produced ductile cast iron (SGI) at different CE and different thickness. The results indicated that, wear for all values of the remaining Mg in the produced SGI decreased as the CE increase at constant thickness and the wear rate increased by increasing cast thicknesses from 20 mm to 80 mm at constant CE %, the minimum wear obtained at CE 3.7 and 20 mm thickness. While, the results indicated that, the total impact energy for the produced SGI increased as the CE increase at constant thickness and the impact energy decreased by increasing cast thicknesses from 20 mm to 80 mm at constant CE %. Moreover, as the pearlite content in the produced SGI increases the wear rate decrease and the total impact energy increase at all values of remaining magnesium.

Keywords—Ductile cast iron, Nodularity, Wear, Impact, and Pearlite matrix.

I. INTRODUCTION

Spheroidal graphite iron (SGI), is one of cast iron type with graphite in spheroidal shape and it is a versatile cast iron revealing a wide range of properties, which are obtained through microstructure control [1, 2]. The most important and characteristic microstructural feature of ductile Iron is the presence of graphite spheres which doing as "crack-arrester" and give ductile iron ductility and toughness higher to all other cast iron types [3-6]. In order to make sure the modularizing process, it is required to use some treatment elements such as magnesium, rare earth elements [7, 8]. But, alloying elements, such as copper, molybdenum, can be useful to alteration the as-cast matrix from ferrite to pearlite. Subsequently, many authors have been done to study the factors that effecting SGI production and to study the properties that existing by nodular cast iron [9-11]. It was found that, the main variables are; chemical composition of the melt, the cooling rate during the solidification, and the types and the amount of nodulizer for liquid metal treatment [12]. SGI provides

at least 80% higher tensile strength, 40% higher elastic modulus and approximately twice the fatigue strength than the other types of cast iron [13]. There are a large number of publications describe the opportunity of obtaining various types of the acicular microstructure [14, 15]. Cast iron's properties are changed by adding various alloying elements, or alloyants. Next to carbon, silicon is the most important alloyant because it forces carbon out of solution. A low percentage of silicon allows carbon to remain in solution forming iron carbide and the production of white cast iron. A high percentage of silicon forces carbon out of solution forming graphite and the production of grey cast iron [18, 19]. Other alloying agents, manganese, chromium, molybdenum, titanium and vanadium counteracts silicon, promotes the retention of carbon, and the formation of those carbides [2, 20, 21]. Nickel and copper increase strength, and machinability, but do not change the amount of graphite formed [22]. The carbon in the form of graphite results in a softer iron, reduces shrinkage, lowers strength, and decreases density [23, 24]. Apart from alloying element and heat treatment graphite nodule size and distribution affects the wear resistance of SG iron. According to a study presence of large size graphite nodules reduces the wear rate by acting as lubricating agent [4, 25]. The main objective of this work is to produce SGI alloys in induction furnace and then to be treated by using different Fe-45Si-5.5Mg nodulizers. The characterization of these alloys was accomplished according to their microstructure, image analyzer, and their mechanical properties; hardness, elongation, tensile and yield strengths to provide technical support for the machine parts, roll mill, roll crushing and automobile applications.

II. EXPERIMENTAL

2.1 Materials

Pig iron, steel scarp, carbon, ferro-silicon, copper, and nodulizer materials are used in this work as shown in table 1. The chemical analysis of these materials was determined by using inductively coupled plasma (ICP) model OES, as shown in Table 3.1.

Table 1 Chemical composition of materials used in this study

Element, % Item	C	Si	Ti	Cu	Mg	Mn
Pig iron	4.2	0.2	0.002	0.002	0.001	0.1
Steel scrap	0.2	0.2	0.001	0.0001	0.000 1	0.01
Carbon	90	-	-	-	-	-
Ferro-silicon	0.5	75	-	-	-	0.2
Copper	-	-	-	99.99	-	-
Nodulizer	0.2	45	-	-	5.6	-

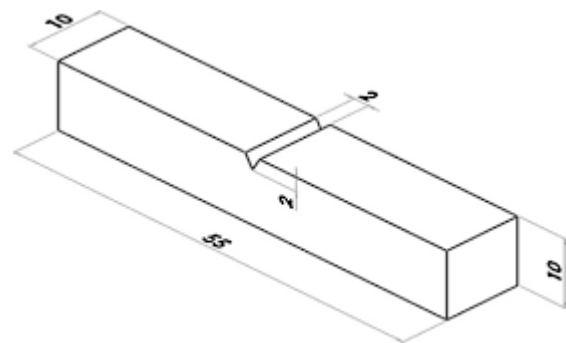
2.2. Procedures

Pig iron and steel scrap weighing about 5 kg charged into an alumina crucible attached in high frequency induction furnace and completely melted, then the flux was added to collect the slag. The slag was skimmed and the molten cast iron was held at an elevated temperature at (1400°C) and a melt sample was taken from the melt to CE meter analysis. Thereafter, the chemical composition was adjusted and checked using the carbon equivalent analyzer. Once the main alloy additions were complete, chilled pieces were taken from each melt for chemical analysis before adding the nodulizer. Liquid treatment, using a Fe–Si–Mg nodulizer was performed by directly injecting the nodulizer into the melt within the pouring ladle., the molten metal was poured into the carbon equivalent analyzer crucible at tapping temperature 1400 °C to estimate the CE, C and Si% after adding the nodulizer. After the desired holding times (1, 4, 7, 10 min) the liquid metal poured into the sand mould and chill mould to produce a sample for chemical analysis. The step sand mould allowed for different section thicknesses Figure 1. Once solidified and cooled to room temperature, the specimens taken from the sand mould and cut for metallographic analysis and mechanical testing. The specimens also were cutting according to ASTM to carry out different mechanical.

Surface of the produced SGI specimens is prepared using standard metallographic techniques before the examination, according to ASTM. After preparation, microstructures of the alloy specimens observed under computerized optical microscope (Model: Olympus BX51). The polished specimens taken for optical microscopy. The microstructures, the shape of graphite (nodularity) and percentage of pearlite of the casting were estimated using software program (SG-3000, Yakamao, Japan) and the results were compared with the standard charts. The samples used for hardness test are prepared need two parallel surfaces polished proceeded as similar of that in microscopic examination. The hardness test carried out using Brinell hardness (load 5 Kgf, $\frac{1}{16}$ inch ball diameter and average of three hardness reading are taken. The standard diameter of the tensile specimen must be 3.125mm and 60mm gage lengths



Figure 1 The Sand mould used in this study



All dimensions in mm

Figure 2 Standard configurations for Charpy (three-point) impact tests

III. RESULTS AND DISCUSSION

3.1 Effect of copper percentage on the pearlite % at different cast thicknesses

Pearlite percentage at different contents of copper (Cu) (ranged between 0.1 and 1 %) at constant CE (4.2%), nodulizer (2.9%), Mn (0.1%), pouring time (2 min.) and different cast thicknesses.

The effect of Cu and cast thickness on the amount of pearlite was investigated using the step mould casting as shown in Figure 1. Figure 3 shows the increasing of Cu in the range from 0.1 to 1.0 % lead to an increase of the volume percent of pearlite for a given cast thickness. At constant Cu contents the pearlite % decrease as cast thickness increased. the increasing the Cu content from 0.1 to 1.0 % resulted in an increase from approximately 33 to 75% pearlite for the 20 mm thick section, and an increase from approximately 28 to 71 % in the 50 mm thick section and an increase from approximately 22 to 62 % in the 80 mm cast thickness. This effect of small Cu

additions on the rise of the spheroidizing phenomena related to the complex processes of segregation of Cu, Mg, and contaminations that are coming from the initial melt and presented by the modifier.

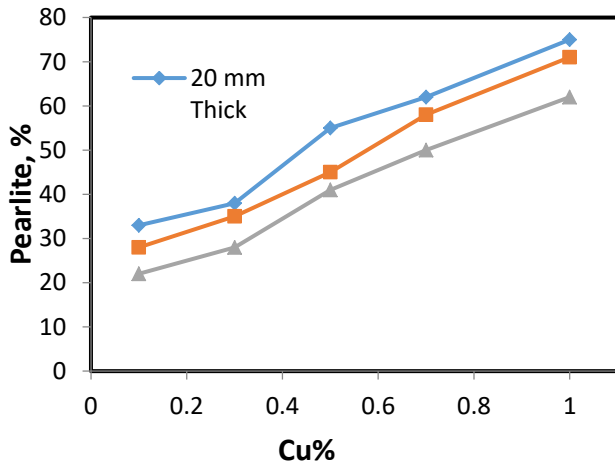


Figure 3 Effect of Cu % on the pearlite % of the produced SGI specimens at different Nodularity.

Figure 4 shows the micrographs of the prepared ductile cast iron containing different amount of pearlite % and Cu contents. All of the samples were taken from the 50 mm cast thickness at different nodularity. The matrix contains carbon in spherical shape (black) surrounded by \square ferrite (white color) within black area (pearlite). The pearlite percentage was measured by software program (SG-3000, Yakamao, Japan). As can be seen the samples contain different amounts of pearlite; 28%, 35%, 58%, and 71% for specimens (a) through (d), respectively. This is confirmed with that published in elsewhere [53, 54]. Moreover, it can be noticed that the nodules size increase with increasing Cu contents in the casts, it might be the presence of Cu hinder the inoculation process.

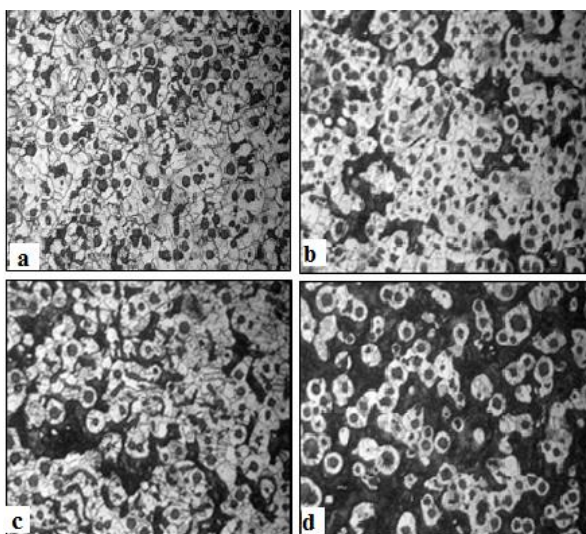


Figure 4 Micrographs of the produced ductile cast iron at different amount of pearlite % and Cu contents (a) (0.1% Cu), 28% pearlite, (b) (0.3% Cu), 35% pearlite, (c) (0.7% Cu), 58% pearlite and (d) (1.0% Cu) 71% pearlite.

3.2 Mechanical Properties of the Produced SGI

Wear rate of SGI alloys at constant CE (4.2 %)

Wear rate of SGI alloys at different contents of residual Mg% (ranged between 0.0155 and 0.031 %) with constant CE (4.2%), Cu (0.15%), Mn (0.15%), pouring time (2 min.) and different thickness of castings is shown in Figure 5.

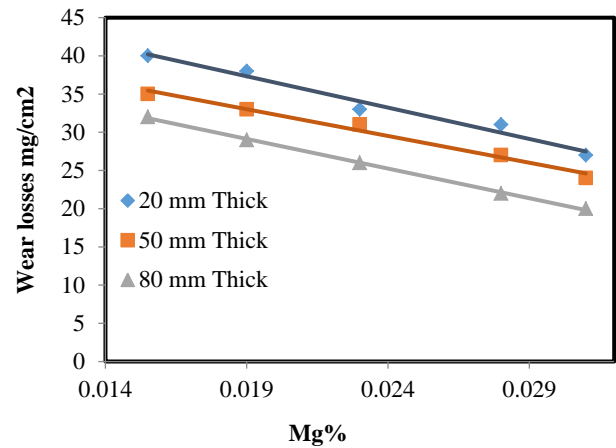


Figure 5 Effect of remaining Mg on the wear losses of the produced SGI specimens at different thicknesses and at constant CE (4.2 %)

Increasing the residual Mg % from 0.0155 to 0.031 % resulted in decreasing the wear rate from 40 to 27 mg/cm² for the 20 mm thick section, from 35 to 24 mg/cm² in the 50 mm thick section and from 32 to 20 mg/cm² in the 80 mm thick section. The Figure indicates that the wear rate decreased with increasing the remaining Mg content at all section thicknesses, due to increasing the nodularity. At any Mg percentage, the wear rate increased with increasing section size due to fast solidification at thin section 20 mm.

Wear rate of SGI alloys at different CE %.

The relation between wear rate and the remaining Mg in the produced casts at thickness 50 mm and at different CE (3.7, 4.2 and 4.7%) as shown in Figure 6. The wear rate is decreased with increasing the remaining Mg%. This result is agreed with the data published elsewhere [34]. In addition, at any remaining Mg, the wear rate is decreased with increasing the CE. The wear rate for the cast thickness 50 mm as a function of the residual Mg could be correlated according to the following equation 1:

$$\text{Wear rate, mg/cm}^2, W = -1391 \text{ Mg\%} + 52.75 \quad (1)$$

Where:

W is the weight loss due to wear at different Mg contents % remaining.

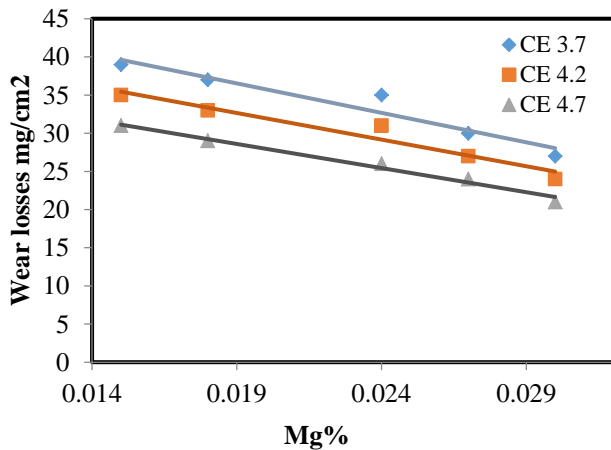


Figure 6 Effect of remaining Mg on the wear losses of the produced SGI specimens at different CE at cast thickness 50 mm.

Effect of pearlite contents on wear in the SGI casts

Effect of Pearlite contents in the produced casts on the Wear at 50 mm thickness, CE 3.7, and Mg 0.031% as indicated in Figure 7. It can be seen that, the weight losses due to wear decrease sharply with increasing pearlite contents in the produced SGI. This is due to increase the hardness of the pearlitic matrix. The Wear amount, mg/cm² was correlated as a function of pearlite% (P) at different cast thickness in the produced SGI as follow:

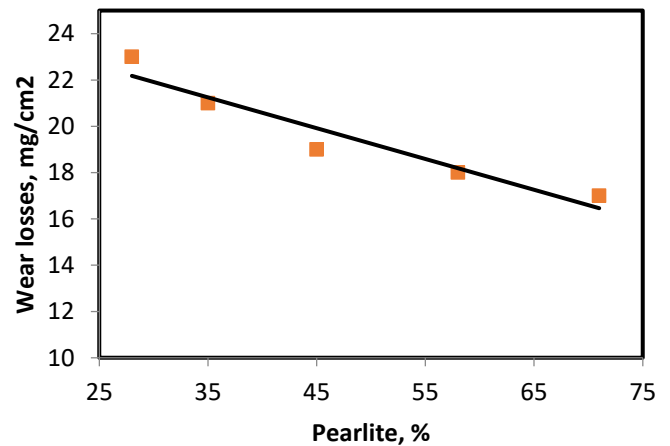


Figure 7 Wear losses of SGI alloys casting, at different Pearlite %.

$$\text{Weight losses, } W, \text{ mg/cm}^2 = 25.901 - 0.1329 P \quad (2)$$

Where:

W is the weight loss due to wear at different pearlite contents, P % remaining.

The wear debris collected from the as-cast SGI is a dark grey color. The wear was carried out using pin-on-disk 2 m/s for 45 min and load 50 N, at different nodularity. The size of most debris are ranged from 2-25 μm, the average particles size of wear debris is increased with decreasing CE% as shown in Fig.8 a-c. The volume, size, morphology and concentration of the wear debris particles produced also are likely to depend on tribological factors such as the properties of the material and the loads and movements experienced at the contact surfaces.

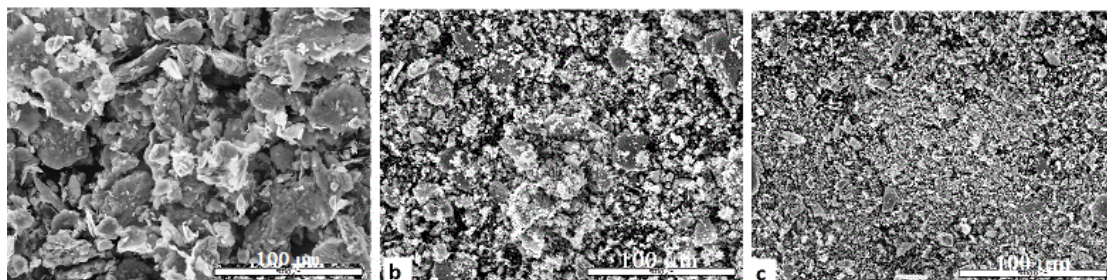


Figure 8 SEM wear debris for SGI castings at different Pearlite contents a) 28 % b) 58 % c) 71 %.

Total impact energy of SGI alloys at constant CE (4.2 %)

The total impact energy of SGI alloys at different contents of remaining Mg% (ranged between 0.0155 and 0.031 %) at constant CE (4.2%), Cu (0.15%), Mn (0.15%), pouring time (4 min.) and different thicknesses of casting is shown in Figure 9. Increasing the residual Mg % from 0.0155 to 0.031 % resulted in an increase of the total impact energy from 12.5 to 21 J for the 20 mm cast thickness, from 11.5 to 19 J in the 50 mm cast thickness and from 10 to 18 J in the 80 mm thick section.

The effect of remaining Mg % at constant CE (4.2 %) on the total impact energy for the SGI samples at different cast thickness of 20, 50 and 80 mm is shown in Figure 9. The total impact energy values increases as the remaining Mg value increase.

Effect of CE on the impact energy of the produced casts

The effect of the remaining Mg % at 50 mm cast thickness on total impact energy for the SGI specimens with different CE of 3.7, 4.2 and 4.7 mm is shown in Figure 10. The total impact energy values were increased with increasing the remaining Mg. In addition, the effect of increasing the carbon

equivalent CE causes decreasing the total impact energy, but the decreasing rate is more at CE 4.7 and this attributed to the cause of decreasing in ductility.

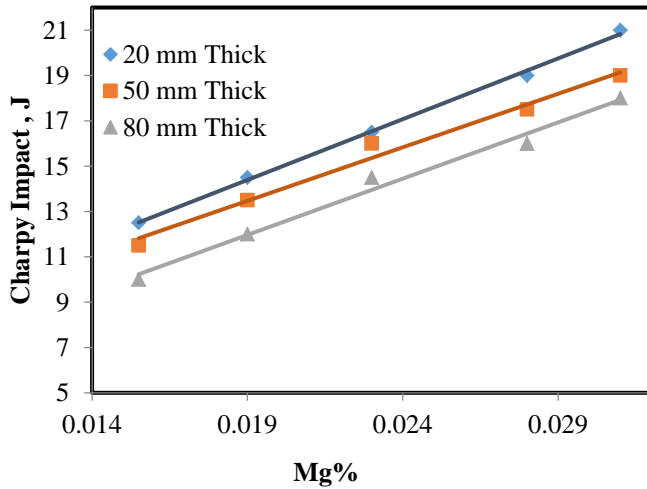


Figure 9 Effect of residual Mg on the impact energy of the produced SGI specimens for constant CE (4.7 %) at different thicknesses

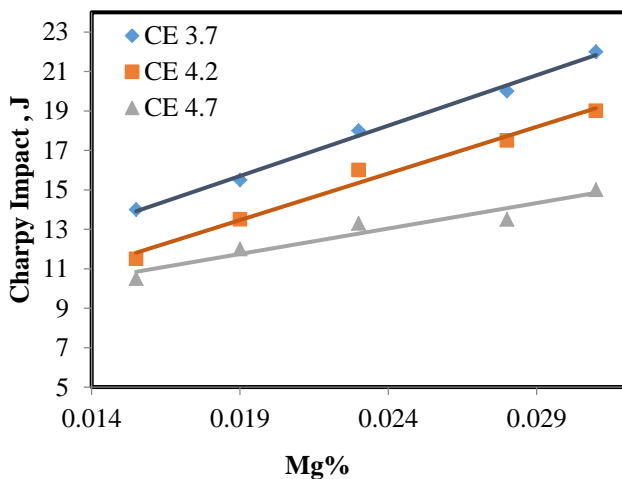


Figure 10 Effect of remaining Mg on total impact energy of the produced SGI castings at different CE and at constant thickness (50 mm). In general, the impact resistance of SGI irons increases by increasing carbon equivalent, and decreases with increasing pearlite. This result is agreed with the data published elsewhere [34].

Effect of pearlite on the impact energy of the produced casts

The total impact energy of SGI alloys at 0.031 % of residual Mg% with constant CE (4.2%), Cu (0.15%), Mn (0.15%), pouring time (4 min.) is shown in Figure 11. Increasing the pearlite contents from 28 to 71 leads to increasing of the total impact energy from 19 to 25 J. The total impact energy values increases as the value of pearlite contents increase. This is due to the increasing of mechanical properties of the casts owning some of toughness.

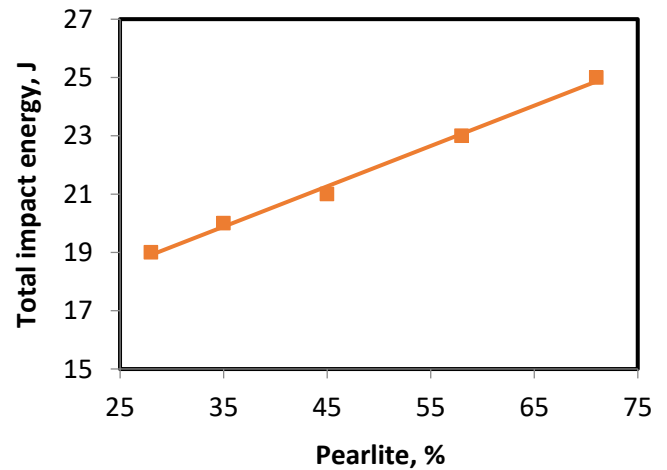


Figure 4.11 The total impact energy of the produced SGI castings at different pearlite contents

For the different types of ductile Iron, the matrix consists of ferrite and pearlite. Ferrite has high ductility, toughness and good machinability, but low hardness and strength and is considered the softest iron phase in ductile Iron. It has high ductility, toughness and good machinability, but low hardness and strength. Pearlite is an entangled mixture of hard lamellar cementite in a ferrite matrix. According to the volume fraction of ferrite and pearlite provides a combination of higher strength and hardness and lower ductility. Therefore, the mechanical properties of ferritic/pearlitic ductile irons are therefore, determined by the ratio of volume fraction of ferrite to pearlite in the matrix. This ratio is controlled in the as-cast form by controlling pearlite stabilizing alloying element such as Cu, Mn and tin which increased the pearlite phase and the cooling rate of the casting [15]

IV. CONCLUSION

From the results and discussion of the present work, the following items can concluded:

1. The wear rate decreased with increasing Mg content for all section thicknesses, also, the wear rate is decreased with increasing the CE.
2. It can be also concluded that, the weight losses due to wear decrease sharply with increasing perlite contents in the produced SGI.
3. In addition, the wear increased with increasing the wear velocity, wear time, and load at different magnesium contents.
4. The total impact energy values increases as the remaining Mg value increase at different cast thicknesses.
5. The effect of decreasing the casts thickness causes increasing the total impact energy.
6. The total impact energy values increases as the value of pearlite contents increase.

REFERENCES

1. H.T. Angus, Cast Iron: Physical and engineering properties. London: Elsevier, 2013.
2. Z. Andrsova and L. Volesky, "The potential of isothermally hardened iron with vermicular graphite", COMAT 2012. 21.-22. 11. 2012. Plzeň, Czech Republic, EU. Retrieved May, 25. 2015 from <http://www.comat.cz/files/-proceedings/11/reports/1060.pdf>, 2012.
3. ASTM, Standard test method for evaluating the microstructure of graphite in iron casting", Designation: A247– 16a, Current edition approved April 1, 2016. Published April 2016. DOI:10.1520/A0247-16A.
4. V K Jh, y H Mozumder, S Sham, R K Beher, A Pattaniak, Sindhoora P, S C Mishra and S Sen, Dry sliding wear system response of ferritic and tempered martensitic ductile iron, Materials Science and Engineering **75** (2015) 012009
5. C. Fragassa, N. Radovic, A. Pavlovic, and G. Minak," Comparison of mechanical properties in compacted and spheroidal graphite irons ", Vol. 38, No. 1 (2016) 45-56, Tribology in Industry www.tribology.fink.rs
6. Sugwon Kim, S.L. Cockcroft , A.M. Omran and Honam Hwang," Mechanical, wear and heat exposure properties of compacted graphite cast iron at elevated temperatures", Journal of Alloys and Compounds 487 (2009) 253–257
7. G. Gumienny, B. Kacprzyk, J. Gawroński, Effect of Copper on the Crystallization Process, Microstructure and Selected Properties of CGI, archives of foundry engineering, 17 (1) (2017) pp51-56
8. R.A.Gonzaga, Influence of ferrite and pearlite content on mechanical properties of ductile cast irons, Materials Science and Engineering: A Volume 567, 1 April 2013, Pages 1-8.
9. Ductile iron data for Design Engineers website: <https://www.ductile.org/didata/Section3/3part1.htm>
10. Jacques lacaze, aline boudot, vale' rie gerval, djar ouab, and Henrique santos, The Role of Manganese and Copper in the Eutectoid Transformation of Spheroidal Graphite Cast Iron, Metallurgical And Materials Transactions A Volume 28A, (1997),pp 2015
11. P. Ferro, A. Fabrizi, R. Cervo, C. Carollo, Journal of Materials Processing Technology, Volume 213, Issue 9, September 2013, Pages 1601-1608.
12. Ductile Iron Society, websit: <http://www.ductile.org/didata/Section2 /2intro.htm#The Casting Advantage>.
13. S.C. Murcia, M.A. Paniagua, E.A. Ossa, Materials Science and Engineering: A, Volume 566, 20 March 2013, Pages 8-15.
14. R. K. Dasgupta, D. K. Mondal, A. K. Chakrabarti, A. C. Ganguli, Journal of Materials Engineering and Performance, August 2012, Volume 21, Issue 8, pp 1728-1736.
15. M. Ramadan, N. El-Bagoury, N. Fathy, M. A. Waly, A. A. Nofal, Journal of Materials Science, June 2011, Volume 46, Issue 11, pp 4013-4019.
16. Marcin Górný, Edward Tyrąła Journal of Materials Engineering and Performance, Volume 22(1) January 2013—300-305.
17. K. Theuwissen, M. Lafont, L. Laffont, B. Viguier, J. Lacaze, Transactions of the Indian Institute of Metals, December 2012, Volume 65, Issue 6, pp 627-631).
18. Serhan karaman, Cem s. Çetinarslan, " Manufacturing process of GGG40 nodular cast iron " International Scientific Conference 19 – 20 november 2010.
19. G. S. Choy, K. H. Choe, K. W. Lee and A. Ikenaga, J. Mater. Sci. Technol., Vol.23 No.1, (2007)97-100.
20. A.M.Omran , G. T. Abdel-Jaber, and M. M. Ali, Effect of Cu and Mn on the Mechanical Properties and Microstructure of Ductile Cast Iron, Int. Journal of Engineering Research and Applications, Vol. 4, Issue 6, June 2014, pp.90-96.
21. Laura D'Agostino, Vittorio Di Cocco, Diego O. Fernandez, Francesco Iacoviello, Damaging micromechanisms in an as cast ferritic and a ferritized ductile cast iron, Procedia Structural Integrity 03 (2017) 201–207.
22. Ioan Milosan, The manufacturing of a special wear-resistant cast iron used in automotive industry, 2nd World Conference On Business, Economics And Management- WCBEM 2013.
23. C. Labrecque¹ and P. M. Cabanne, Low temperature impact strength of heavy section ductile iron castings: effects of microstructure and chemical composition, China foundry Vol 8 No 1(3011).
24. Glavas, Z., Lisjak, D., and Unkcic, F., "The application of artificial neural network in the prediction of the as-cast impact toughness of spheroidal graphite cast iron", Kovove Mater., Vol. 45, 2007, p. 41–49.
25. Irena Zmak Tomislav Filetin, Mechanical Properties of Ductile Cast Iron Determined by Neural Networks, Proceedings of the Third International Conference on Modeling, Simulation and Applied Optimization Sharjah,U.A.E January 20-22 2009.